Supplemental Material for Garbincius et al., Enhanced NCLX-dependent mitochondrial Ca^{2+} efflux attenuates pathological remodeling in heart failure

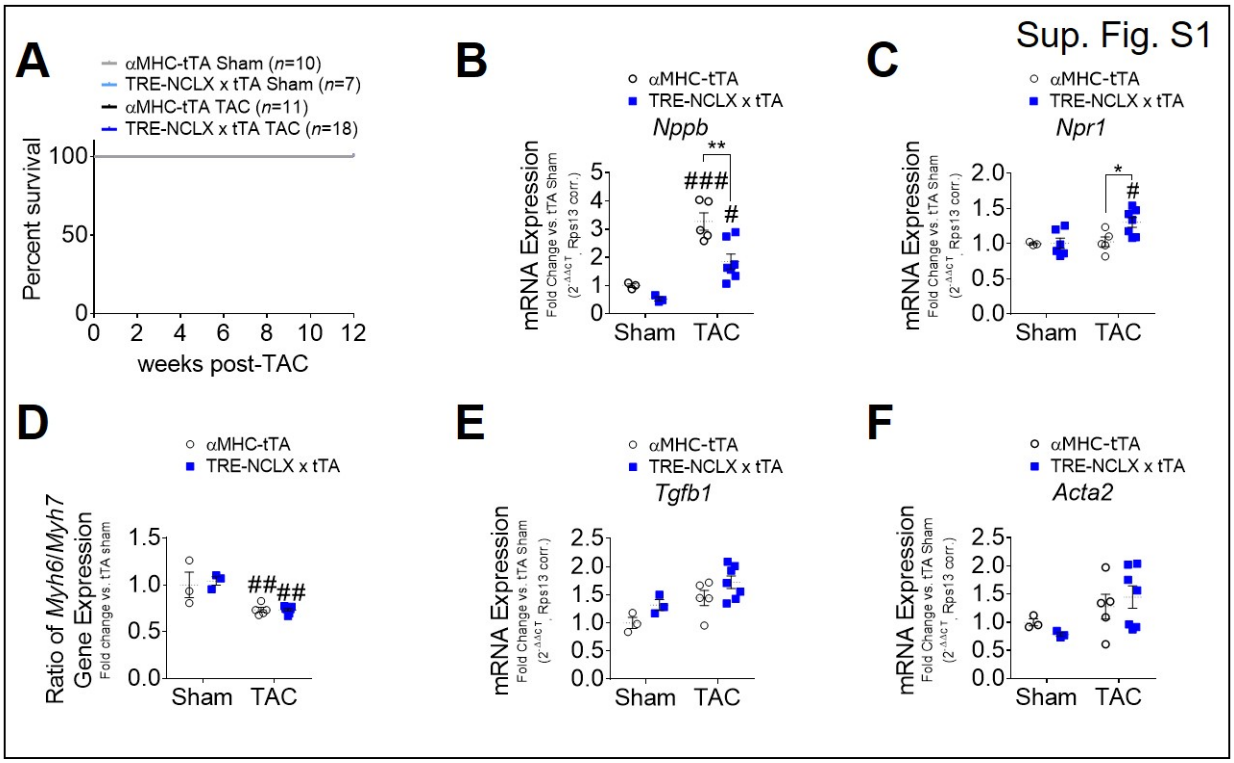

Supplemental Figure S1: Related to Fig. 1, Cardiomyocyte-specific NCLX overexpression protects against pressure overload-induced HF and pathological remodeling. **A**) Kaplan-Meier survival curve of αMHC-tTA and TRE-NCLX x αMHC-tTA mice for 12 weeks after sham or TAC surgeries. The number of animals in each group at the start of the study is indicated in parentheses. Data analyzed by log-rank (Mantel-Cox) test. qPCR quantification of mRNA expression of fetal (**B**-**D**) and pro-fibrotic (**E**-**F**) genes in hearts of αMHC-tTA and TRE-NCLX x αMHC-tTA mice 12 weeks after sham or TAC surgeries. *Nppb*, natriuretic peptide type B; *Npr1*, natriuretic peptide receptor 1; *Myh6*, α-myosin heavy chain; *Myh7*, β-myosin heavy chain; *Tfgb1*, transforming growth factor β-1; *Acta2*, α-smooth muscle actin. Data analyzed by 2-way ANOVA with Sidak's post-hoc test. $^{\#}P<0.05$, $^{\#\#}P<0.01$, $^{\#\#\#}P<0.001$ vs. sham; $^{*}P < 0.05$, $^{**}P < 0.01$ αMHC-tTA vs. TRE-NCLX x αMHC-tTA. (*n*=3-7 mice/group).

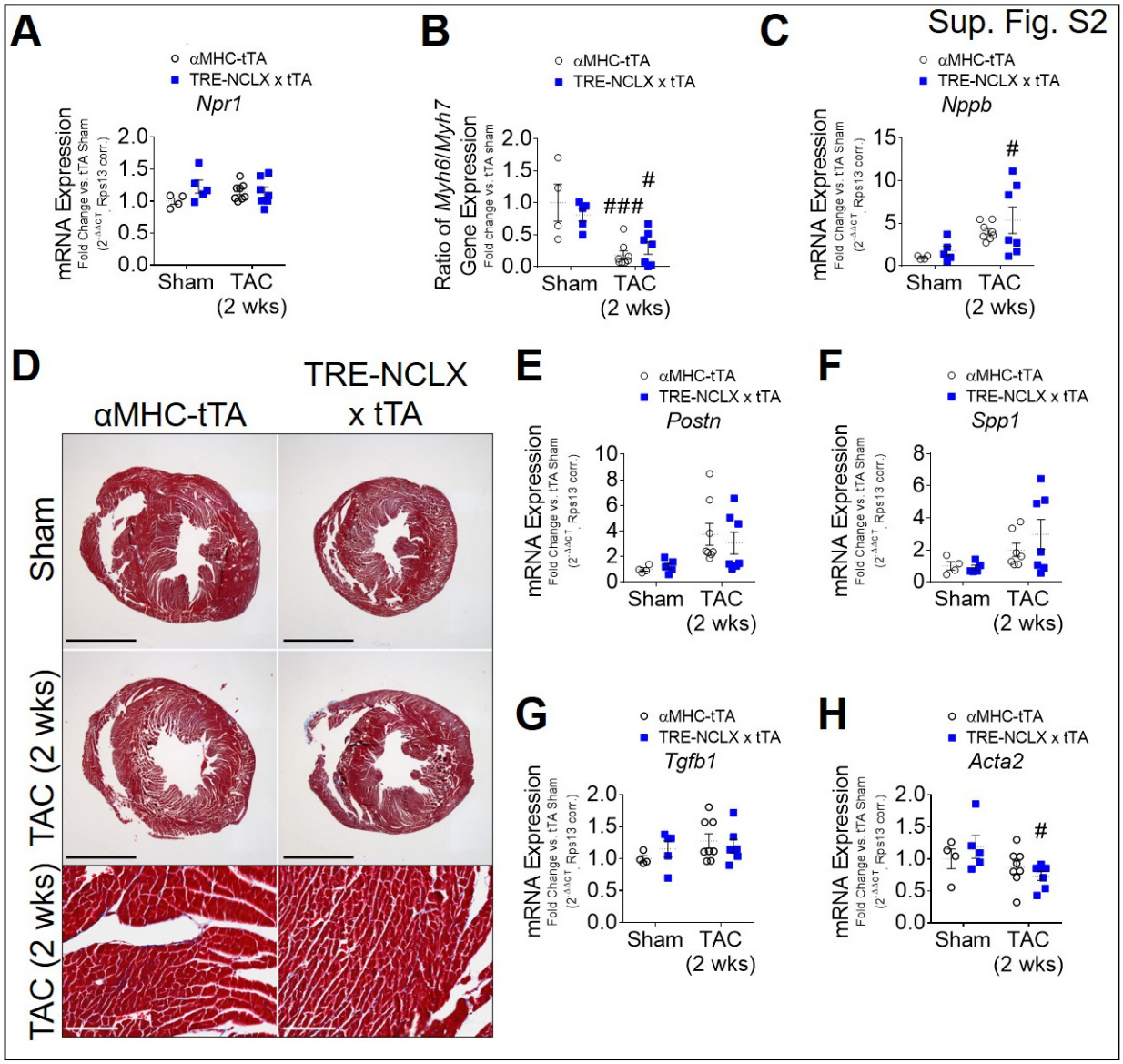

Supplemental Figure S2: Related to Fig. 2, Cardiomyocyte NCLX overexpression attenuates early pressure overload-induced cardiac hypertrophy. A-C) qPCR quantification of mRNA expression of fetal genes in hearts of αMHC-tTA and TRE-NCLX x αMHC-tTA mice 2 weeks after sham or TAC surgeries. *Npr1*, natriuretic peptide receptor 1; *Myh6*, α-myosin heavy chain; *Myh7*, β-myosin heavy chain; *Nppb*, natriuretic peptide type B. Data analyzed by 2-way ANOVA with Sidak's post-hoc test. $^{\#}P<0.05$, $^{\#\#\#\#}P<0.0001$ vs. sham. (n=4-8 mice/group). **D**) Representative images of Masson's trichrome stain for myocardial collagen deposition (blue) at 2 weeks post-surgery. Black scale bars for whole-heart cross sections = 2mm. White scale bars for higher magnification micrographs (bottom row) = 100 µm. **E-H**) qPCR quantification of mRNA expression of pro-fibrotic genes in hearts of mice 2 weeks after sham or TAC surgeries. *Postn*, periostin; *Spp1*, osteopontin; *Tfgb1*, transforming growth factor β-1; *Acta2*, α-smooth muscle actin. Data analyzed by 2-way ANOVA with Sidak's post-hoc test. $^{\#}P<0.05$ vs. sham. (n=4-8 mice/group).

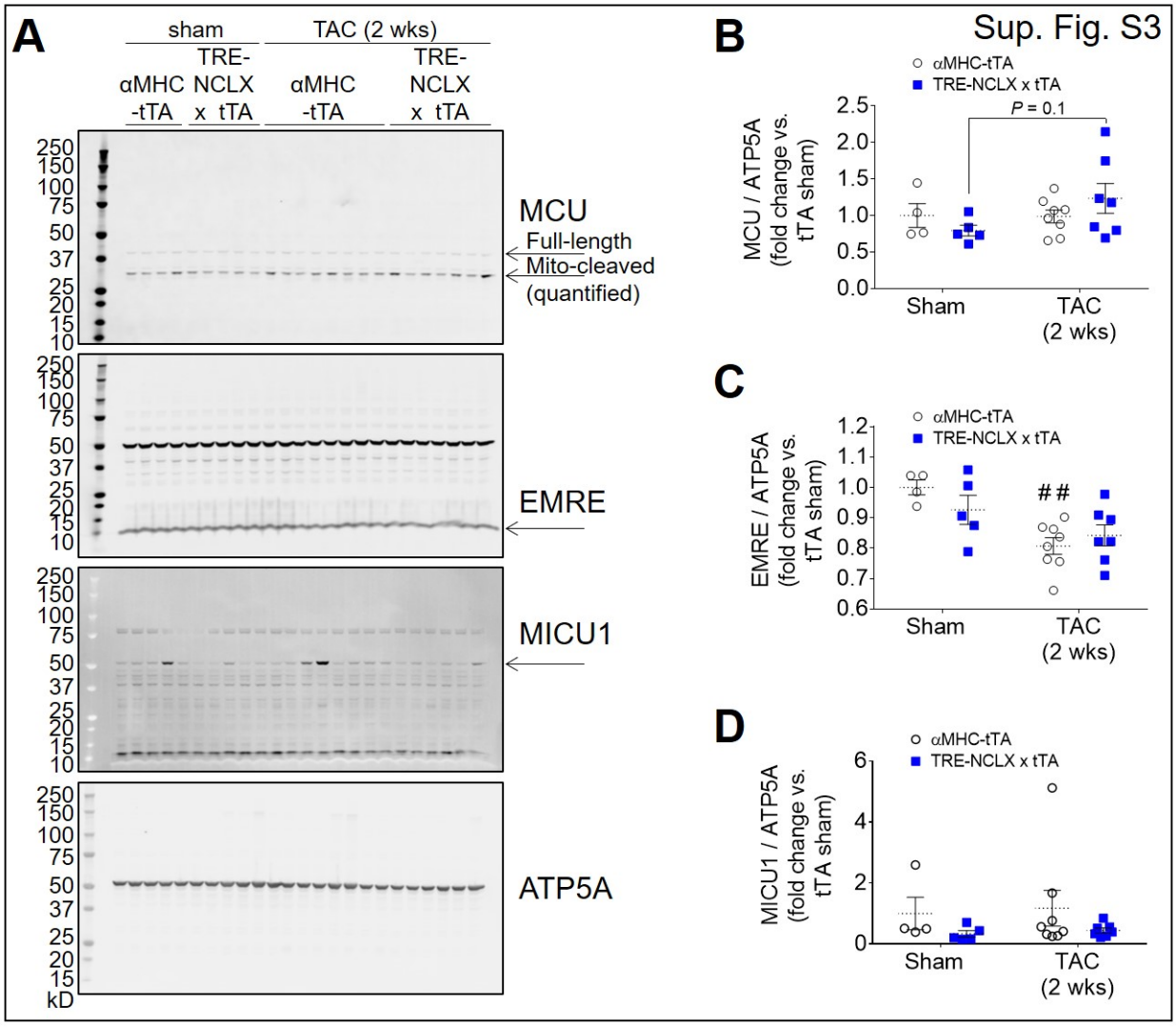

Supplemental Figure S3: mtCU component expression related to Fig. 2 - Cardiomyocyte NCLX overexpression attenuates early pressure overload-induced cardiac hypertrophy. **A**) Full-length western blots for mitochondrial calcium uniporter channel components MCU, EMRE, and MICU1, and mitochondrial loading control ATP5A, in hearts of αMHC-tTA and TRE-NCLX x αMHC-tTA mice at 2 weeks post sham or TAC surgery. Arrows indicated analyzed bands. Quantification of MCU (**B**), EMRE (**C**), and MICU1 (**D**) expression normalized to mitochondrial loading control ATP5A. Data analyzed by 2-way ANOVA with Sidak's post-hoc test. $^{\#\#}P<0.01$ vs. sham. (n=4-8 mice / group).

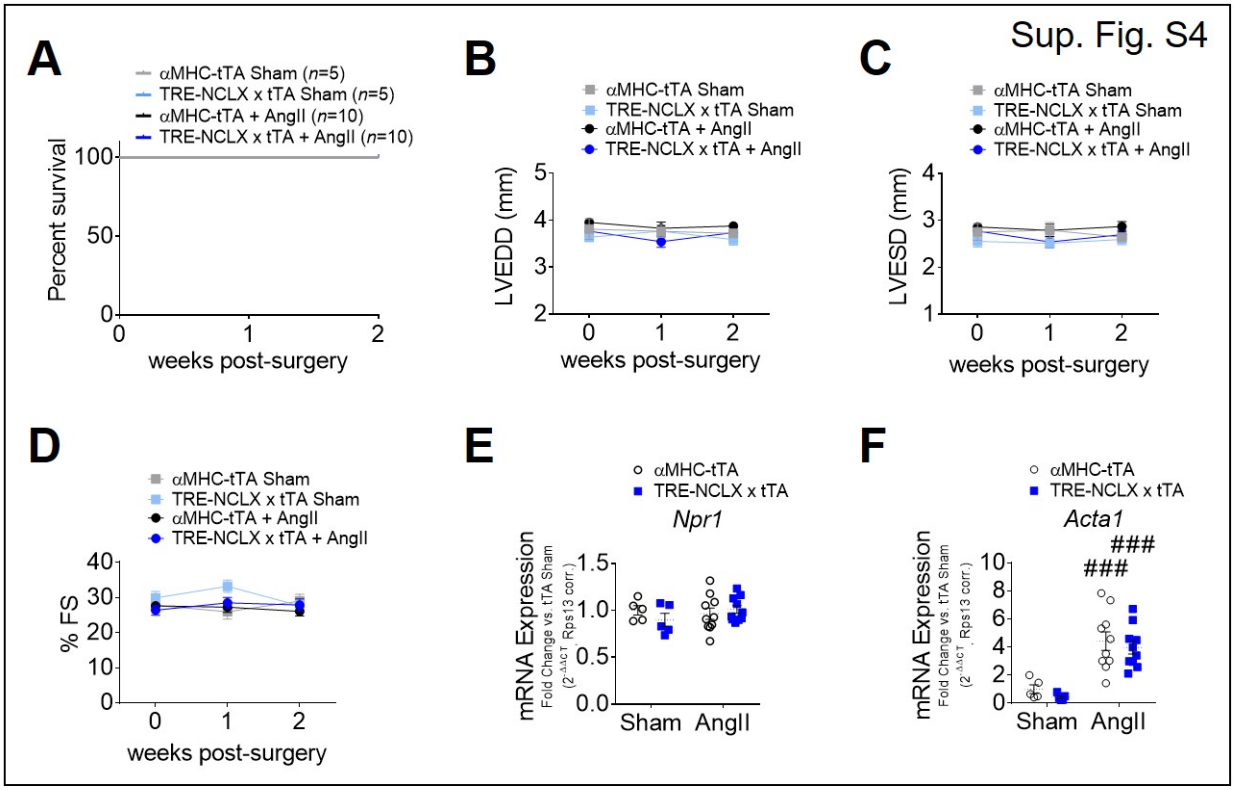

Supplemental Figure S4: Related to Fig. 3 - Cardiomyocyte NCLX overexpression attenuates hypertrophy in mice infused with angiotensin II. A) Kaplan-Meier survival curve of αMHC-tTA and TRE-NCLX x αMHC-tTA mice for 2 weeks after sham or angiotensin II osmotic minipump implantation surgeries. The number of animals in each group at the start of the study is indicated in parentheses. Data analyzed by log-rank (Mantel-Cox) test. Left ventricular end diastolic dimension (LVEDD) (**B**), end systolic dimension (LVESD) (**C**), and percent fractional shortening (%FS) (**D**) in αMHC-tTA and TRE-NCLX x αMHC-tTA mice over 2 weeks of low-dose angiotensin II (AngII) infusion. Data analyzed by 2-way ANOVA with Tukey's post-hoc test. (*n*=5-10 mice / group). **E-F**) qPCR quantification of mRNA expression of fetal genes in hearts of αMHC-tTA and TRE-NCLX x αMHC-tTA mice 2 weeks after sham or angiotensin II minipump implantation surgery. *Npr1*, natriuretic peptide receptor 1; *Acta1*, α-skeletal muscle actin. Data analyzed by 2-way ANOVA with Sidak's post-hoc test. $^{\#\#\#}P<0.001$ vs. sham. (*n*=5-10 mice / group).

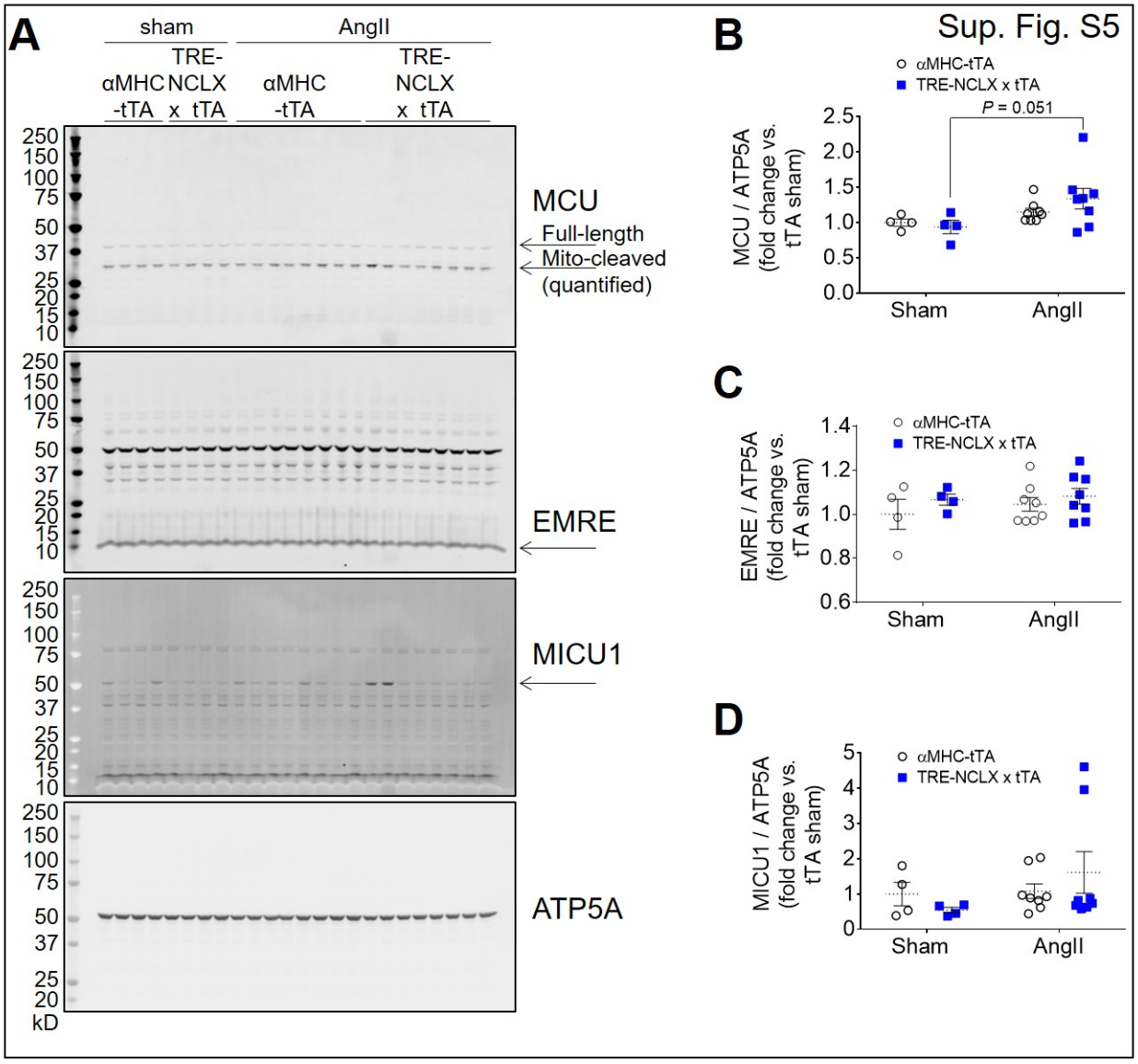

Supplemental Figure S5: mtCU component expression related to related to Fig. 3 - Cardiomyocyte NCLX overexpression attenuates hypertrophy in mice infused with angiotensin II. A) Full-length western blots for mitochondrial calcium uniporter channel components MCU, EMRE, and MICU1, and mitochondrial loading control ATP5A, in hearts of αMHC-tTA and TRE-NCLX x αMHC-tTA mice after 2 weeks post- sham or AngII minipump implantation surgery. Arrows indicated analyzed bands. Quantification of MCU (**B**), EMRE (**C**), and MICU1 (**D**) expression normalized to mitochondrial loading control ATP5A. Data analyzed by 2-way ANOVA with Sidak's post-hoc test. (*n*=4-8 mice / group).

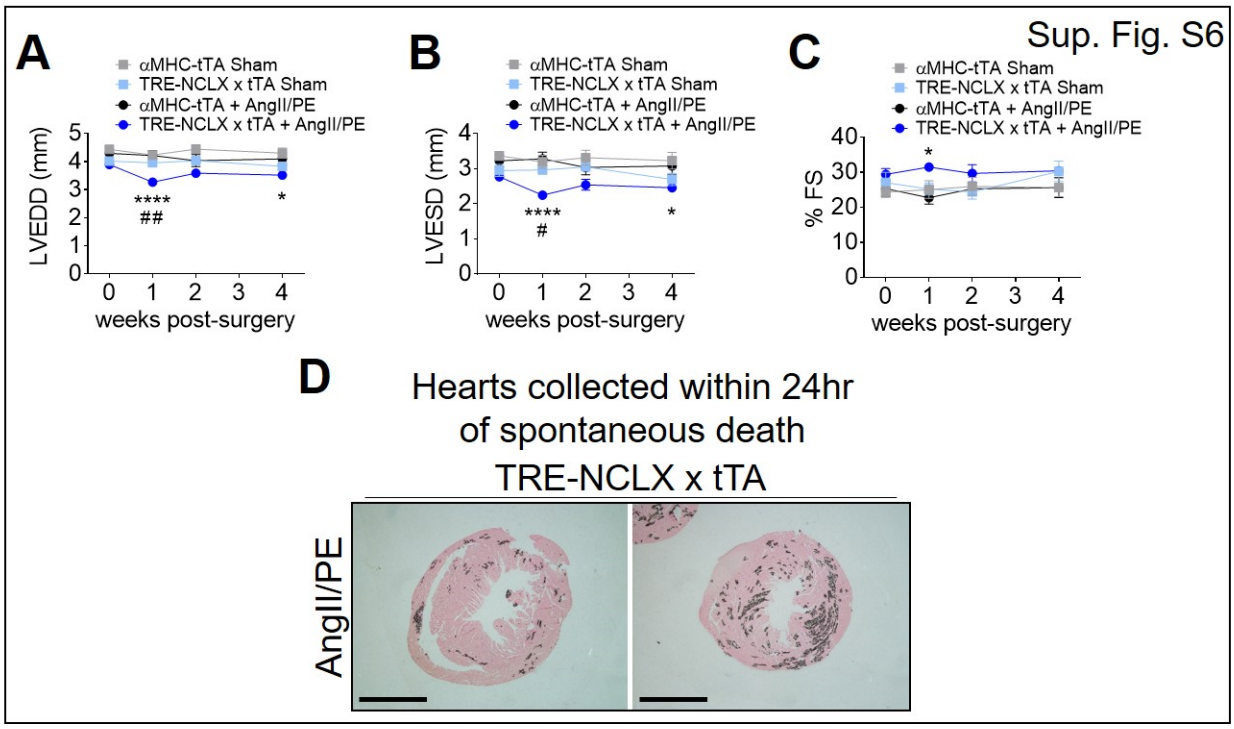

Supplemental Figure S6: Related to Fig. 4 - Cardiomyocyte NCLX overexpression attenuates remodeling but reduces survival in mice infused with chronic high-dose angiotensin II + phenylephrine. Left ventricular end diastolic dimension (LVEDD) (**A**), end systolic dimension (LVESD) (**B**), and percent fractional shortening (%FS) (**C**) in αMHC-tTA and TRE-NCLX x αMHC-tTA mice over 4 weeks of high-dose AngII/PE infusion. Data analyzed by 2-way ANOVA with Tukey's post-hoc test. **P*<0.05, *****P*<0.0001 αMHC-tTA + AngII/PE vs. TRE-NCLX x αMHC-tTA + AngII/PE; $^{\#}$*P*<0.05, $^{\#\#}$*P*<0.01 TRE-NCLX x αMHC-tTA + AngII/PE vs. sham. (*n*=6-17 mice / group). **D**) Observational finding of von Kossa staining for Ca^{2+}-precipitant deposition (black) in the hearts of two TRE-NCLX x αMHC-tTA hearts that died spontaneously within the first two weeks following AngII/PE minipump implantation surgery. Scale bars = 2mm.

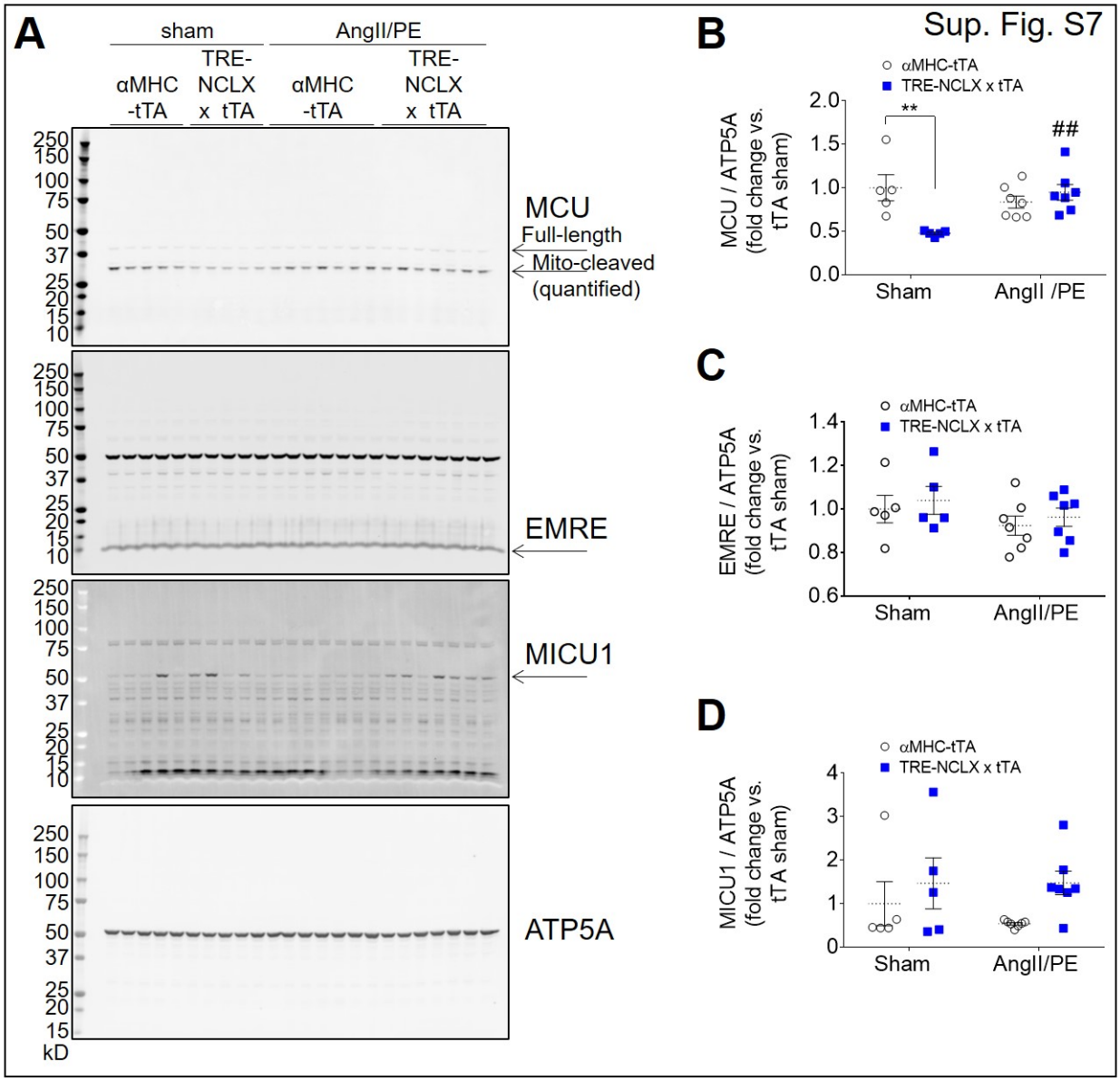

Supplemental Figure S7: mtCU component expression related to related to Fig. 4 - Cardiomyocyte NCLX overexpression attenuates remodeling but reduces survival in mice infused with chronic high-dose angiotensin II + phenylephrine. A) Full-length western blots for mitochondrial calcium uniporter channel components MCU, EMRE, and MICU1, and mitochondrial loading control ATP5A, in hearts of αMHC-tTA and TRE-NCLX x αMHC-tTA mice after 4 weeks post- sham or AngII/PE minipump implantation surgery. Arrows indicated analyzed bands. Quantification of MCU (**B**), EMRE (**C**), and MICU1 (**D**) expression normalized to mitochondrial loading control ATP5A. Data analyzed by 2-way ANOVA with Sidak's post-hoc test. $^{\#\#}P<0.01$ vs. sham; $^{**}P<0.01$ αMHC-tTA vs. TRE-NCLX x αMHC-tTA. (n=5-7 mice / group).

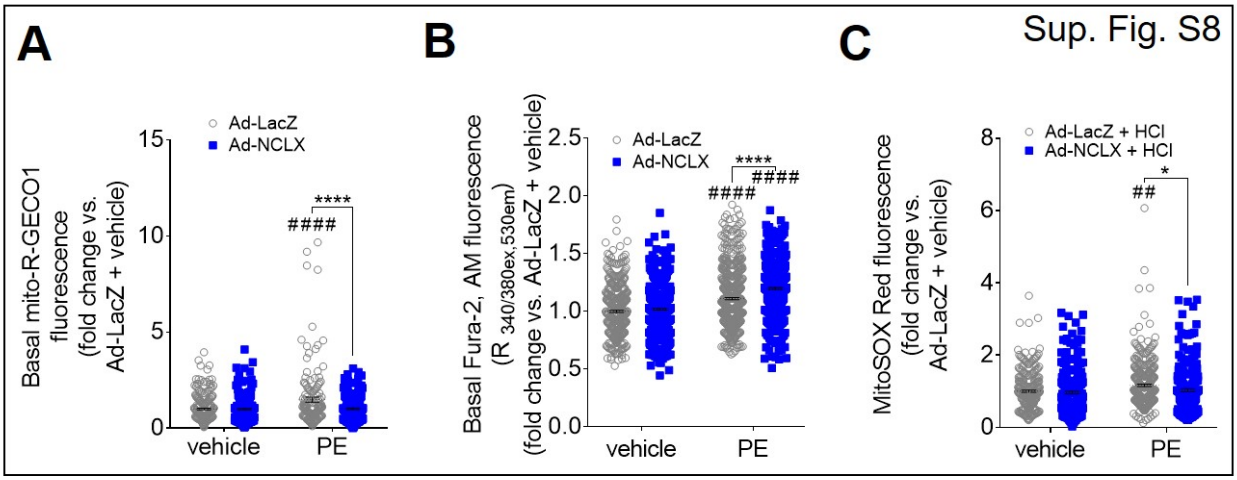

Supplemental Figure S8: Related to Fig. 5 - NCLX expression limits oxidative capacity and biosynthetic potential of cardiomyocytes during hypertrophic stimulation *in vitro*. A) Basal, steady-state $_{m}Ca^{2+}$ content in neonatal rat ventricular myocytes (NRVMs) transduced with adenovirus encoding β-galactosidase (Ad-LacZ) or human NCLX (Ad-NCLX) and treated with vehicle or phenylephrine (PE), as indicated by fluorescence of the genetically-encoded mitochondrial Ca^{2+} reporter, mito-R-GECO1. Data analyzed by 2-way ANOVA with Sidak's post-hoc test. $^{\#\#\#\#}P<0.0001$ vs. vehicle; $^{****}P<0.0001$ Ad-LacZ vs. Ad-NCLX. (n = 248 cells for Ad-LacZ + vehicle; 247 cells for Ad-NCLX + vehicle; 149 cells for Ad-LacZ + PE; 207 cells for Ad-NCLX + PE). Graph depicts individual data points corresponding to the summary bar graph shown in Fig. 5A. **B**) Basal, steady-state cytosolic Ca^{2+} level in NRVMs, as indicated by fluorescence of the ratiometric Ca^{2+} reporter dye, Fura-2, AM. Data analyzed by 2-way ANOVA with Sidak's post-hoc test. $^{\#\#\#\#}P<0.0001$ vs. vehicle; $^{****}P<0.0001$ Ad-LacZ vs. Ad-NCLX. (n = 507 cells for Ad-LacZ + vehicle; 567 cells for Ad-NCLX + vehicle; 598 cells for Ad-LacZ + PE; 542 cells for Ad-NCLX + PE). Graph depicts individual data points corresponding to the summary bar graph shown in Fig. 5B. **C**) Mitochondrial superoxide production in NRVMs, as indicated by fluorescence of the dye MitoSOX Red. Data analyzed by 2-way ANOVA with Sidak's post-hoc test. $^{\#\#}P<0.01$ vs. vehicle; $^{*}P<0.05$ Ad-LacZ vs. Ad-NCLX. (n = 252 cells for Ad-LacZ + vehicle; 261 cells for Ad-NCLX + vehicle; 379 cells for Ad-LacZ + PE; 249 cells for Ad-NCLX + PE). Graph depicts individual data points corresponding to the summary bar graph shown in Fig. 5C.

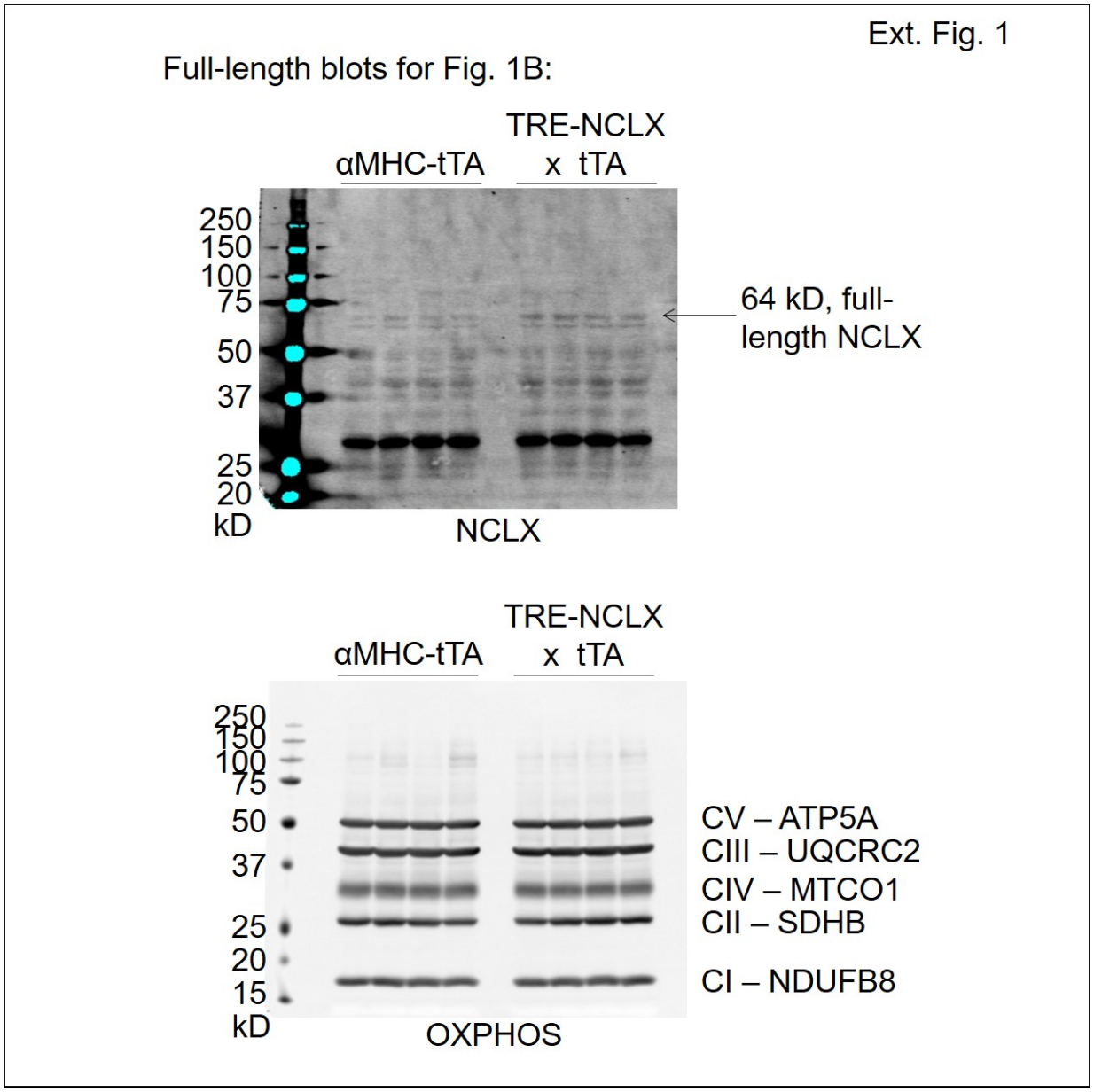

Extended Figure 1: Full-length blots for Figure 1B. Arrow indicates full-length NCLX.

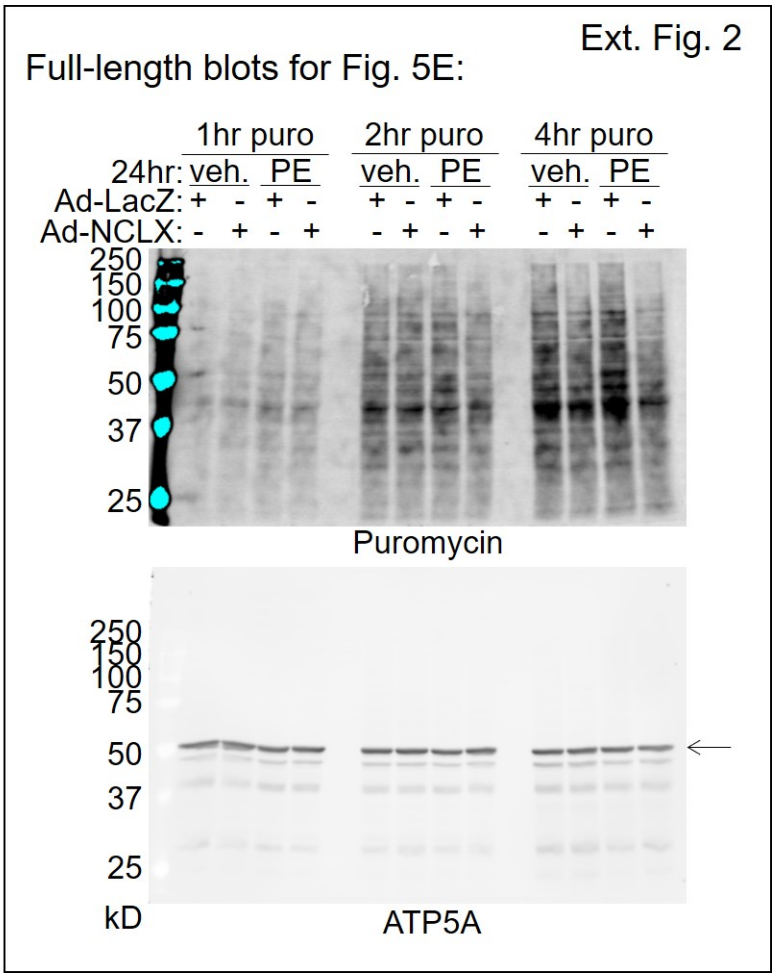

Extended Figure 2: Full-length blots for Figure 5E. Arrow indicates ATP5A band.